Roles of defects and grain sizes in photoluminescence of nanocrystalline SrTiO$_3$

Roles of defects and grain sizes in photoluminescence of nanocrystalline SrTiO$_3$

W F Zhang†, Z Yin†, M S Zhang†, Z L Du‡ and W C Chen§

† National Laboratory of Solid State Microstructures, Centre for Materials Analysis, and
Department of Physics, Nanjing University, Nanjing 210093, People's Republic of China
‡ Department of Physics, Henan University, Kaifeng 475001, People's Republic of China
§ Institute of Physics, Sinica, Academia, Beijing 100080, People's Republic of China

E-mail: `mszhang@netra.nju.edu.cn`

Abstract. Nanocrystalline SrTiO$_3$ was prepared by a stearic acid sol–gel technique. X-ray measurements showed that the sample obtained is of good quality and the grain sizes range from 26 to 120 nm. One blue photoluminescence (PL) band at around 470 nm was observed at room temperature. Investigation of the dependence of the visible emission band on annealing temperatures and grain sizes showed that the effects of grain size and dielectric confinement play important roles, and that oxygen vacancies may act as the radiative centres responsible for the observed visible emission band. The mechanism for the luminescence is explained within the framework of self-trapped excitons.

1. Introduction

Size effects in ferroelectric materials have become a subject of increasing interest recently. Decreasing dimension in microelectronic and optoelectronic devices requires knowledge of material properties below a critical size. In particular, effects of grain size are well known to play an important role in changing the ferroelectricity, phase transitions, and optical properties in ABO$_3$ perovskite-type oxides [1–3]. Strontium titanate (SrTiO$_3$) has long attracted considerable attention due to its excellent dielectric, piezoelectric, and photoelectric properties [4–7]. Photoluminescence (PL) spectroscopy is one of the most powerful techniques for studying physical properties such as the electronic structure of SrTiO$_3$. PL from single-crystal SrTiO$_3$ has been studied extensively. At low temperatures it shows one broad and structureless visible emission band at around 500 nm upon excitation with ultraviolet radiation, while above 110 K, this band is almost quenched [7, 8]. Using time-resolved spectroscopy, Leonelli and Brebner [9, 10] attributed the visible emission to the recombination of self-trapped excitons (STEs), and considered the highly localized sensitization centres to be the traps capturing electrons or holes in the formation of STEs. The luminescence resulting from the STE recombination was also observed in BaTiO$_3$, MgTiO$_3$, anatase TiO$_2$, and other titanates [11, 12]. Recently, a broad-band visible emission, as a function of grain size, has been observed at room temperature in nanocrystalline SrTiO$_3$ and BaTiO$_3$ [13]. The dependence of the emission efficiency and energy maximum on the grain size showed that the surface states might be the dominant cause for the observed visible emission.

In bulk and nanocrystalline $SrTiO_3$ materials, impurities and crystal defects greatly influence the electrical and optical properties. Moreover, the optical properties of nanometre-sized, direct- or indirect-band-gap, semiconductors is an area of fundamental and technical interest. For example, visible luminescence of the semiconductor nanoparticles like those of CdS, Ge/GeO_2, and Si/SiO_2 has been reported [14–16]. Therefore, PL study of nanocrystalline $SrTiO_3$ (nc-$SrTiO_3$) is of rather apparent significance. In this paper we report a blue PL band in nc-$SrTiO_3$ prepared by a stearic acid sol–gel technique. The PL behaviours and mechanism are discussed in terms of effects of nanometre size, dielectric confinement, and thermal annealing.

2. Experimental procedure

Nanocrystalline $SrTiO_3$ samples were prepared starting from strontium stearate, tetrabutyl titanate, and stearic acid. First, the metal-containing compounds were dissolved in molten stearic acid (70 °C). Second, the resulting transparent solution upon cooling transformed into the dry gel, which was heat treated at 750 °C for 4 h in air to form white nc-$SrTiO_3$ powders. To change the concentration of defect states and achieve various grain sizes, the powders obtained were annealed for 1 h at different temperatures from 500 to 1000 °C in air. The chemical phase and the crystal structure of these powders were examined using x-ray diffraction (XRD) (Rigaku, Cu Kα). Their average grain sizes were calculated from the XRD patterns via the classical Scherrer equation [17], $D = k\lambda/\beta(\theta)\cos\theta$, where D is the average grain diameter, k the constant (shape factor about 0.9), λ the x-ray wavelength, $\beta(\theta)$ the full width at half-maximum (FWHM) of the diffraction line, and θ the diffraction angle.

PL measurements were performed using a fluorescence spectrometer (Spex F212) where a xenon lamp with 150 mW output was used as the excitation source and the width of each of the four slits was set at 2 mm. In order to facilitate the PL measurements and to ensure the same experimental conditions for the different samples, the as-prepared powders were compressed into pellets 12 mm in diameter and 0.8 mm in thickness, which have the same density (2.52 g cm^{-3}). The position of the pellet was kept unchanged in the measurements.

3. Results and discussion

Figure 1(a) shows the XRD pattern of the unannealed sample, indicating a monophase cubic structure in the nc-$SrTiO_3$. Shown in figure 1(b) is the change of the (110) diffraction lineshape (intensity and linewidth) with increasing annealing temperature. The decrease in linewidth and the increase in intensity of the diffraction line for the increased annealing temperatures show that the grain size of the nc-$SrTiO_3$ increases with increasing annealing temperature. The FWHM value of the diffraction line obtained from the Lorentzian fitting includes errors from the apparatus conditions such as the noise and the slit width of the x-ray diffractometer. These errors were removed by subtracting the FWHM value of the single-crystal $SrTiO_3$(100) diffraction line. The FWHM values calibrated, as a function of the annealing temperature, are clearly shown in figure 1(c), from which we obtain the following data: for the unannealed sample the grain size is 26 nm, and for the samples annealed at 500, 600, 700, 800 and 1000 °C, the grain size is 26.8, 27.3, 28.6, 40 and 120 nm, respectively.

The PL emission and excitation spectra for the unannealed sample are shown in figure 2, where the excitation spectrum was recorded for emission at 490 nm and has its maximum at 398 nm. Under excitation at 398 nm, the unannealed sample gives a room-temperature blue emission band centred at 470 nm. For comparison, the PL spectrum of single-crystal $SrTiO_3$ measured is also presented in figure 2. It is seen that the single-crystal $SrTiO_3$ emits very weak
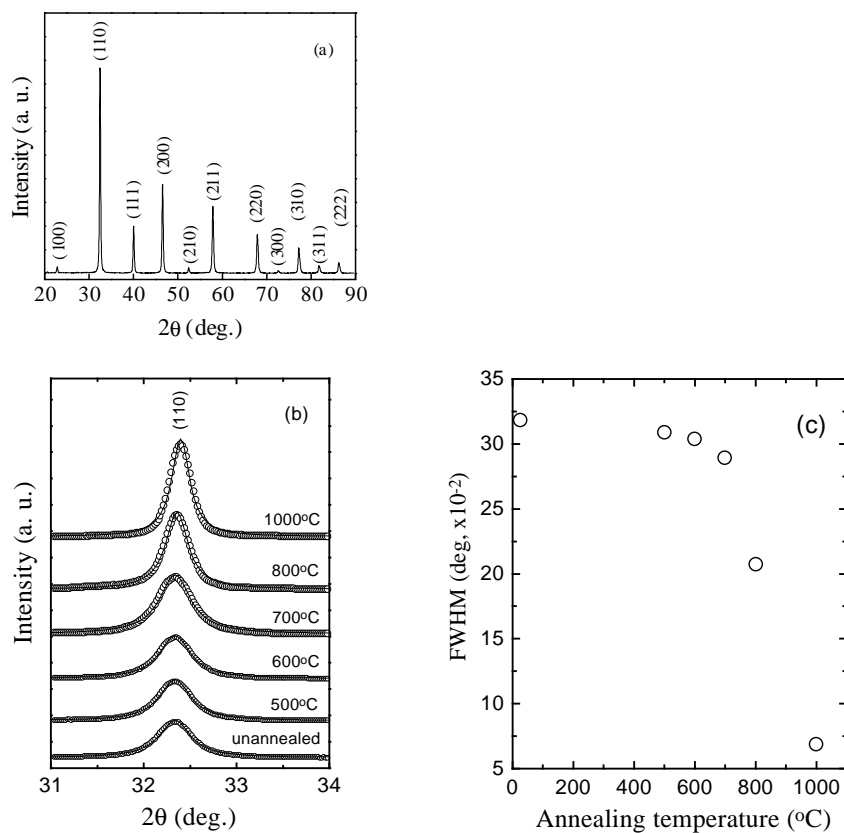
Figure 1. (a) The x-ray diffraction pattern of the unannealed nc-SrTiO$_3$ sample. (b) Lineshapes of (110) peaks at various annealing temperatures; solid curves stand for the Lorentzian fits. (c) FWHM values of (110) peaks as a function of annealing temperature.
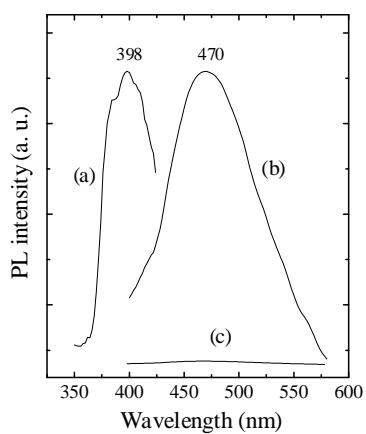

Figure 2. The PL excitation spectrum (a) and emission spectrum (b) of the unannealed nc-SrTiO$_3$. Excitation and emission spectra were recorded for emission at 490 nm and excitation at 398 nm, respectively. Curve (c) shows the PL emission spectrum of single-crystal SrTiO$_3$.

luminescence, whereas the PL in the nc-SrTiO$_3$ is strong at room temperature.

It is known that there exist three types of additional energy levels in the forbidden band of titanates: free-exciton levels, STE levels, and defect or impurity levels [18]. All of them are near to the conduction band. The band gap of single-crystal SrTiO$_3$ has been determined to be between 3.2 and 3.4 eV [19]. According to the data from photoacoustic spectroscopy measurements [20], the band gap is about 3.5 eV for the nc-SrTiO$_3$ of grain size 26 nm. The excitation energy used in the present work (3.1 eV corresponding to 398 nm) is lower than the band gap (3.5 eV), so it is difficult for an electron in the valence band to be directly excited to the conduction band; however, it is likely to be excited to the localized levels within the forbidden gap. Therefore, the observed broad-band PL does not result from the free-exciton recombination. The free-exciton emission is usually caused by a band-gap excitation and has a narrow-band feature. In fact, for titanate materials it has been found only in rutile TiO$_3$ single crystals at low temperatures.

This visible emission band is not associated with any particular impurities, since it is independent of the preparation method and process conditions [13]. In other poly- and nano-crystalline oxides, oxygen vacancies are known to be the most common defects and usually act as radiative centres in luminescence processes [21–23]. The energy difference (0.46 eV) between the excitation and the emission indicates a strong relaxation of the exciton. SrTiO$_3$ is a polar dielectric material; the strong coupling between the lattice and the electronic part of the excitons would result in the self-trapping of excitons [9]. On the basis of the luminescence mechanism in single-crystal SrTiO$_3$ and the above discussion, the origin of this blue PL band can be well explained with the aid of the STE model. That is, electrons in the valence band are excited to some localized levels by absorbing incident photons and form small polarons, and holes in the conduction band interact with the polarons to form STEs. The recombination of the STEs leads to the blue emission.

On the basis of the size effect of excitons in nc-Si discussed by Takagahara and Takeda [24], it is assumed that the binding energy and the radiative lifetime of STEs are strongly related to grain sizes. The efficient STE luminescence found recently in neutral fullerene C$_{60}$ [25] seems to exhibit the size effect of STEs. In single-crystal SrTiO$_3$, it is difficult to detect the STE luminescence at room temperature as a result of the small binding energy and the short radiative lifetime of STEs. In the nc-SrTiO$_3$, however, the binding energy and the radiative lifetime of STEs are greatly enhanced. The spatial overlap between the envelope functions of electrons and holes increases with decreasing grain size, leading to the enhancement of the STE binding energy. Furthermore, the enhanced STE binding energy may prolong the STE radiative lifetime. Meanwhile, the dielectric confinement effect also enhances the binding energy because of the penetration of the electric force lines between electrons and holes into the surrounding medium [26]. Also, the dielectric confinement effect would become stronger in small-sized SrTiO$_3$ which has a high dielectric constant. The small-sized particles can introduce more opportunity for the electric force lines to penetrate into the surrounding medium with relatively low dielectric constant with respect to the bulk materials. As for the naked SrTiO$_3$ nanoparticles surrounded by air with a very low dielectric constant, the dielectric confinement effect is certainly remarkable. It is believed, therefore, that STEs in the nc-SrTiO$_3$ have strong binding energy and long radiative lifetime, and that their recombination causes the room-temperature PL. And obviously, the PL intensity would decrease with increasing grain size.

To achieve a further understanding of the mechanism of the luminescence in the nc-SrTiO$_3$, PL measurements for the samples annealed at various temperatures were performed. Figures 3 and 4 show their PL spectra as functions of annealing temperature and grain size. It is seen clearly that the PL intensity increases as the annealing temperature increases up to 700 °C,

indicating the increase of the STE concentration. It is noted that the grain size increases slightly with increasing annealing temperature below 700 °C, as shown in figure 4. This small change in grain size is believed to have less influence on the STE concentration, so the increase of the PL intensity should be mainly due to the increase in the number of oxygen vacancies acting as radiative centres in the samples. When the annealing temperature goes up, the concentration of the oxygen vacancies and thus of STEs increases; the STE recombination is consequently enhanced. Finally, the PL intensity increases with increasing annealing temperature. Above 700 °C, however, the PL intensity starts to drop, and almost disappears for the sample annealed at 1000 °C. The increase of the concentration of oxygen vacancies and thus of electron–hole pairs generated by absorbing photons with increasing annealing temperature does not always lead to the increase of the STE concentration, because the STE formation from the electron–hole pairs depends on the grain size. That is, the oxygen vacancies and the grain sizes determine the STE concentration cooperatively. It is seen from figure 4 that the grain size increases rapidly above 700 °C; so the influence of the grain size on the concentration of STEs should be expected to prevail over that of the oxygen vacancies. Above 700 °C, therefore, the STE concentration and thereby the PL intensity decreases with increasing annealing temperature. Figure 3 also shows that the spectral lineshapes remain unchanged and the PL peak positions have no detectable shifts for various annealing temperatures.
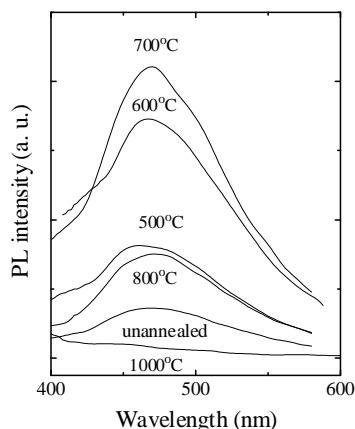

Figure 3. The annealing temperature dependence of the PL emission spectra for nc-SrTiO$_3$.
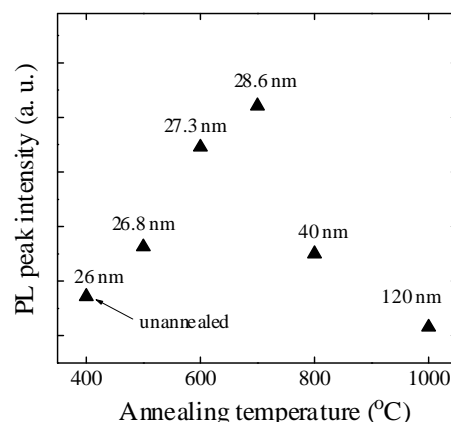

Figure 4. PL peak intensity as a function of both annealing temperature and grain size. The grain sizes are marked in the figure.

Finally, let us discuss other possible origins for the observed PL. In the case of nanocrystals, surface states are often regarded as the dominant cause of the luminescence, since there are a large number of unsaturated atoms existing in the surface region of the nanometre crystallites and forming localized levels within the forbidden gaps of materials. In the literature [13], the mechanism related to surface states was used to account for the increase in intensity of the luminescence and the blue-shift in the energy maximum with decrease of grain size. However, it does not seem to explain the PL intensity increase with increasing annealing temperature observed in the present work. Therefore, the nanometre-size effect and the oxygen vacancies could play a dominant role in the luminescence processes. It should be mentioned that the spectral shape for the nc-SrTiO$_3$ is very similar to that of single-crystal SrTiO$_3$—that is, they behave as broad and structureless visible emission bands. This also shows that the luminescence in the nanocrystals and in single crystals would seem to have the same radiative

process via the STE recombination. And the oxygen vacancies may be considered to be the highly localized sensitization centres in the nc-SrTiO$_3$. In addition, it is worth noting that in the present study the strong PL was observed in the cubic nc-SrTiO$_3$ at room temperature, whereas in the literature [7–9] the reported luminescence was all from the tetragonal phase of single-crystal SrTiO$_3$ at temperatures below 110 K, where a phase transition from tetragonal to cubic structure occurs. This shows that the luminescence quenching above 110 K could not be attributed to the tetragonal–cubic phase transition of SrTiO$_3$. The study of a relation between the luminescence and the phase structure in nc-SrTiO$_3$ is under way.

4. Conclusions

A strong blue PL band has been revealed in the nc-SrTiO$_3$ prepared by a sol–gel technique. The origin for the PL band is well explained by the model of self-trapped excitons associated with oxygen vacancies. The effects of both the grain size and the dielectric confinement enhance the binding energy and the radiative lifetime of STEs in the nc-SrTiO$_3$, leading to the room-temperature PL. The critical annealing temperature is found to be 700 °C. Below and above 700 °C, oxygen vacancies and grain sizes are the dominant cause of the blue PL band, respectively.

Acknowledgments

References

[1] Sartirena M R, Multani M S, Ayyub P and Vijayaraghavan R 1983 *Ferroelectrics* **52** 137
[2] Meng J F, Zou G T, Cui Q L, Zhao Y N and Zhu Z Q 1994 *J. Phys.: Condens. Matter* **6** 6543
[3] Chattopadhyay S, Ayyub P, Palkar V R and Multani M 1995 *Phys. Rev.* B **52** 13 177
[4] Qu B D, Evstigneev M, Johnson D J and Prince R H 1998 *Appl. Phys. Lett.* **72** 1394
[5] Grupp D E and Goldman A M 1997 *Science* **276** 392
[6] Courths R, Noffke J, Wern H and Heise R 1990 *Phys. Rev.* B **42** 9127
[7] Feng T 1982 *Phys. Rev.* B **25** 627
[8] Grabner L 1968 *Phys. Rev.* **177** 1315
[9] Leonelli R and Brebner J L 1985 *Solid State Commun.* **54** 505
[10] Leonelli R and Brebner J L 1986 *Phys. Rev.* B **33** 8649
[11] Aguilar M, Gonzalo C and Godefroy G 1980 *Ferroelectrics* **25** 467
[12] De Haart L G J, De Vries A J and Blasse G 1985 *J. Solid State Chem.* **59** 291
[13] Meng J F, Huang Y B, Zhang W F, Du Z L, Zhu Z Q and Zou G T 1995 *Phys. Lett.* A **205** 72
[14] Chestnoy N, Harris T D, Hull R and Brus L E 1986 *J. Phys. Chem.* **90** 3393
[15] Zacharias M and Fauchet P M 1997 *Appl. Phys. Lett.* **71** 380
[16] Tsybeskov L, Hirschman K D, Duttagupta S P, Zacharias M, Fauchet P M, McCaffrey J P and Lockwood D J 1998 *Appl. Phys. Lett.* **72** 43
[17] Ishikawa K, Yoshikawa K and Ukada N 1988 *Phys. Rev.* B **37** 5852
[18] De Haart L G J and Blasse G 1986 *J. Solid State Chem.* **61** 135
[19] Capizzi M and Frova A 1970 *Phys. Rev. Lett.* **25** 1298
[20] Zhou L, Zhang S Y, Fu S W, Wang Z and Zhang L D 1997 *J. Phys.* **46** 994 (in Chinese)
[21] Vanheusden K, Warren W L, Voigt J A, Seager C H and Tallant D R 1995 *Appl. Phys. Lett.* **67** 1280
[22] Foress L and Schubnell M 1993 *Appl. Phys.* B **56** 363
[23] Zhu Y C, Ding C X, Ma G H and Du Z L 1998 *J. Solid State Chem.* **139** 124
[24] Takagahara T and Takeda K 1992 *Phys. Rev.* B **46** 15 578
[25] Matus M, Kuzmany H and Sohmen E 1992 *Phys. Rev. Lett.* **68** 2822
[26] Takagahara T 1993 *Phys. Rev.* B **47** 4569